Initial State Anisotropies in Ultra-Central collisions of Deformed Nuclei

April 6th 2022

N. Fortier, S. Jeon and C. Gale

compute canada | calcul canada

QUARK MATTER KRAKÓW 2022

McGill UNIVERSITY

Our Model

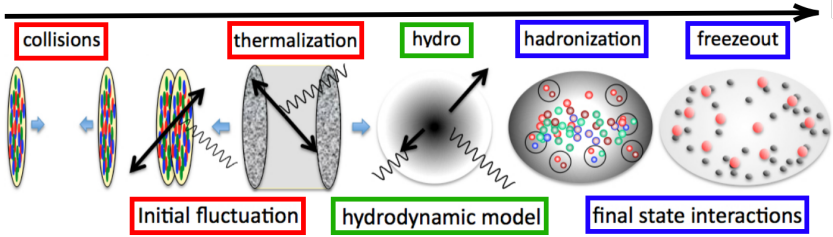

- IP-Glasma: boost-invariant saturation-based model (strong classical gluon fields, CGC) (Schenke, Tribedy, Venugopalan, PRL 108, 252301 (2012))
- MUSIC: 2+1D Relativistic viscous hydrodynamics (Schenke, Jeon, Gale, PRC 82, 014903 (2010))
- iS3D+UrQMD: Cooper-Frye Monte Carlo particle sampling + hadronic transport, interactions and final state resolution (McNelis, Everett, Heinz, arXiv 1912, 08271 (2019) & Bass, Belkacem, Bleicher et al., PPNP 41, 225-370 (1998))

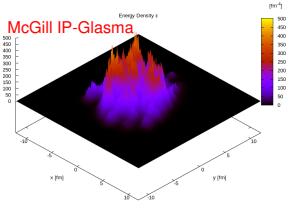

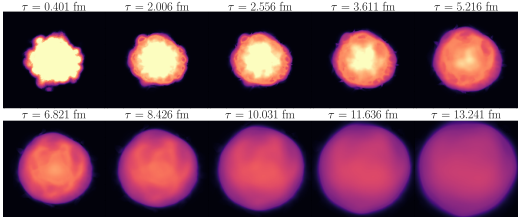

Sample MUSIC evolution, from $\tau = 0.4$ fm to 13 fm

Why Collide Deformed Nuclei?

- **Non-trivial initial geometries in ultra-central regime**
  - Elliptic flow (v_2)
  - Skewed p_T distributions
  - Jet quenching
- Diversity in initial matter distributions at $b \approx 0$ fm
- Test understanding of multiplicity-generating mechanisms

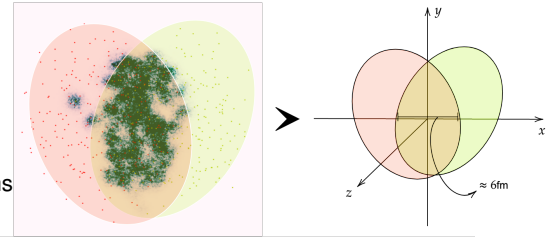

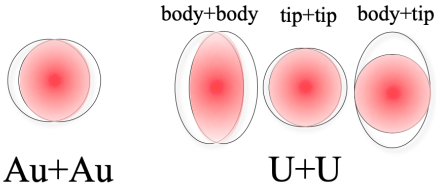

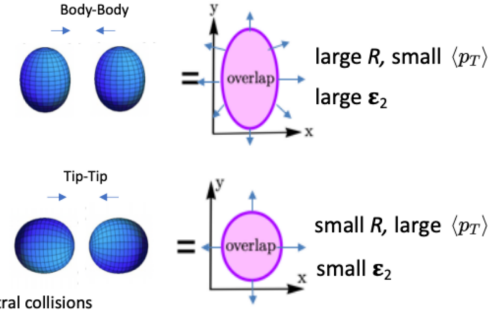

Figure from Giacalone, PRL 124, 202301 (2020)

Results A

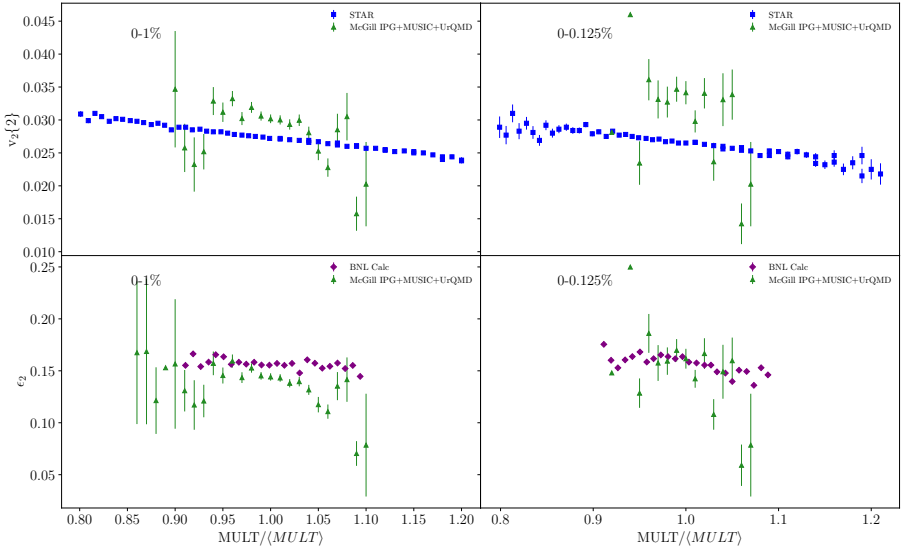

Figure 1A: 2-particle elliptic flow and eccentricity vs. scaled multiplicity ($|\eta| < 1$, $0.2 \leq p_T \leq 2.0$ GeV)

Results A

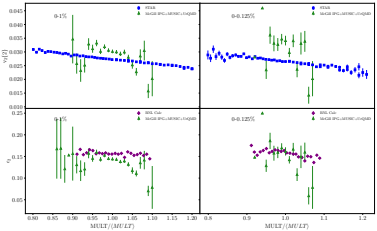

Figure 1A: 2-particle elliptic flow and eccentricity vs. scaled multiplicity

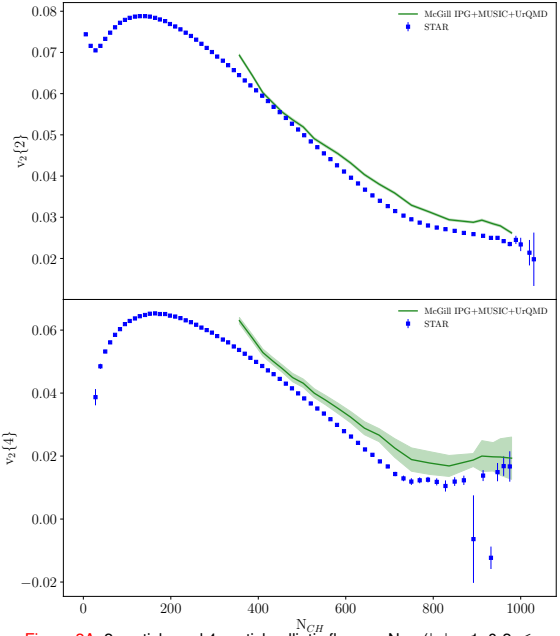

Figure 2A: 2-particle and 4-particle elliptic flow vs. N_{CH} ($|\eta| < 1$, $0.2 \leq p_T \leq 2.0$ GeV)

Results A

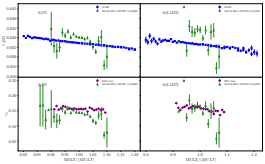

Figure 1A: 2-particle elliptic flow and eccentricity vs. scaled multiplicity

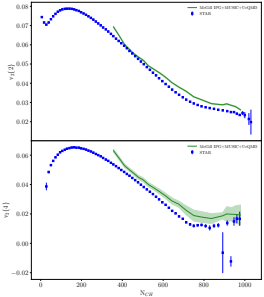

Figure 2A: 2-particle and 4-particle elliptic flow vs. charged particle multiplicity

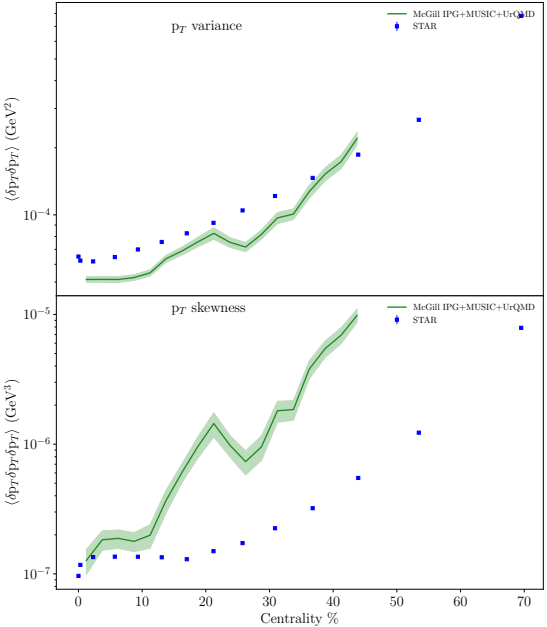

Figure 3A: p_T distribution variance and skewness vs. centrality ($|\eta| < 1$, $0.2 \leq p_T \leq 2.0$ GeV)

Results B

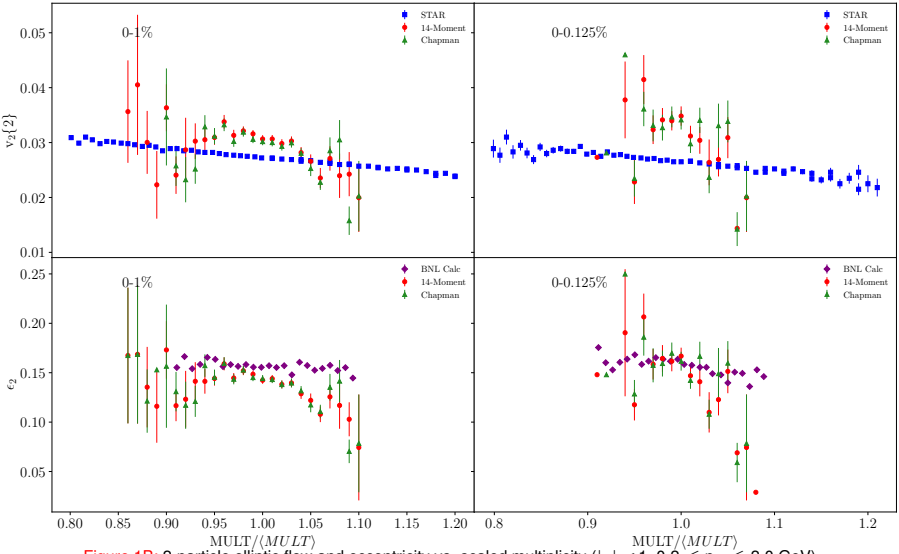

Figure 1B: 2-particle elliptic flow and eccentricity vs. scaled multiplicity ($|\eta| < 1$, $0.2 \leq p_T \leq 2.0$ GeV)

Results B

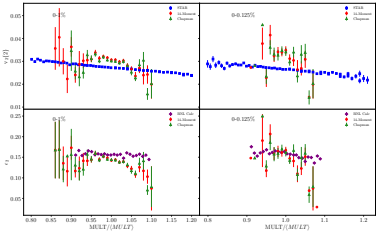

Figure 1B: 2-particle elliptic flow and eccentricity vs. scaled multiplicity

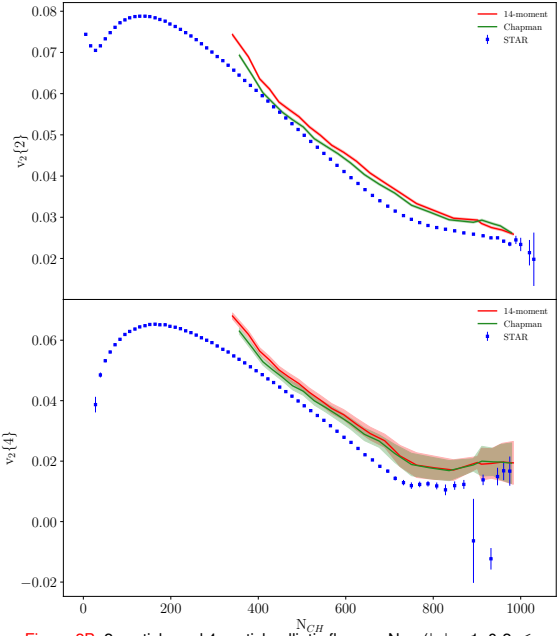

Figure 2B: 2-particle and 4-particle elliptic flow vs. N_{CH} ($|\eta| < 1$, $0.2 \leq p_T \leq 2.0$ GeV)

Results B

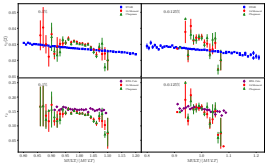

Figure 1B: 2-particle elliptic flow and eccentricity vs. scaled multiplicity

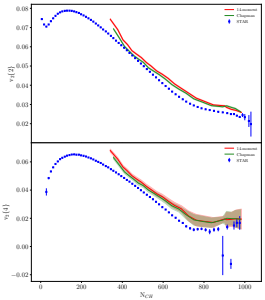

Figure 2B: 2-particle and 4-particle elliptic flow vs. charged particle multiplicity

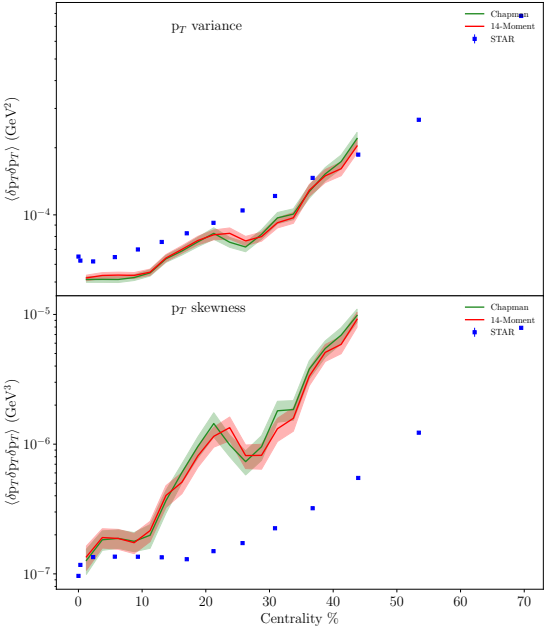

Figure 3B: p_T distribution variance and skewness vs. centrality ($|\eta| < 1$, $0.2 \leq p_T \leq 2.0$ GeV)

Conclusion & Next Steps

Conclusion

- Presented results from the first comprehensive v_2 and p_T analysis of initial state + hydro + hadronic cascade simluations of deformed systems at $\sqrt{s} = 193$ GeV
- IP-Glasma's QCD-based approach is successful at reproducing key observables of deformed systems, especially in the ultra-central regime, thanks to
  - Initial state fluctuations
  - Pre-equilibrium flow
  - Multiplicity dependence on $Q_S^2 S_\perp$
- Our data shows that the unique geometry of deformed systems has a large effect on key observables
- p_T distributions are robust to changes in δf correction

Next Steps

- Analyze full set of observables to further compare 14-moment and Chapman-Enskog δf correction
- Select events in 10-30% centrality and determine if lattice artifacts in hydro phase are a factor
- Compute and release identified particle spectra

Backup

Chapman-Enskog vs. 14-moment

Both are popular methods of linearizing the phase-space distribution function $f_n(x,p)$ around its equilibrium $f_{eq,n}$, which is relevant since it appears in the **Cooper-Frye formula**

$$E_p \frac{dN_n}{d^3p} = \frac{1}{(2\pi\hbar)^3} \int_\Sigma p \cdot d^3\sigma(x) f_n(x,p)$$

Chapman-Enskog

Boltzmann-based gradient expansion which uses RTA

$$\delta f_n = -\frac{p \cdot \partial f_{eq,n}}{p \cdot u/\tau_r}$$

Conservation of net baryon number, energy & momentum are applied together with the first-order Navier-Stokes relations

$$\delta f_n = f_{eq,n}\bar{f}_{eq,n}\left[\frac{\Pi}{\beta_\Pi}\left(b_n\mathcal{G} + \frac{(u\cdot p)\mathcal{F}}{T^2} + \frac{(-p\cdot\Delta\cdot p)}{3(u\cdot p)T}\right)\right.$$

$$\left.\frac{V_B^\mu p_{\langle\mu\rangle}}{\beta_V}\left(\frac{n_B}{\mathcal{E}+\mathcal{P}_{eq}} - \frac{b_n}{(u\cdot p)}\right) + \frac{\pi_{\mu\nu}p^{\langle\mu\rangle}p^{\langle\nu\rangle}}{2\beta_\pi(u\cdot p)T}\right]$$

Coefficients are adjusted to reproduce $T^{\mu\nu}$

14-moment

Truncated at hydro level (p^μ & $p^\mu p^\nu$)

$$\delta f_n = f_{eq,n}\bar{f}_{eq,n}\left(b_n c_\mu p^\mu + c_{\mu\nu}p^{\mu\nu}\right)$$

Assume c_μ&$c_{\mu\nu}$ to be species independent

$$\delta f_n = f_{eq,n}\bar{f}_{eq,n}\left(c_T m_n^2 + b_n\left(c_B(u\cdot p) + c_V^{\langle\mu\rangle}p_{\langle\mu\rangle}\right)\right.$$

$$\left.+c_E(u\cdot p)^2 + c_Q^{\langle\mu\rangle}(u\cdot p)p_{\langle\mu\rangle} + c_\pi^{\langle\mu\nu\rangle}p_{\langle\mu\rangle}p_{\langle\nu\rangle}\right)$$

Fix coefficients s.t. Landau matching condition is respected and they reproduce $\pi^{\mu\nu}$, Π and V_B^μ

Comparing WS Parametrizations

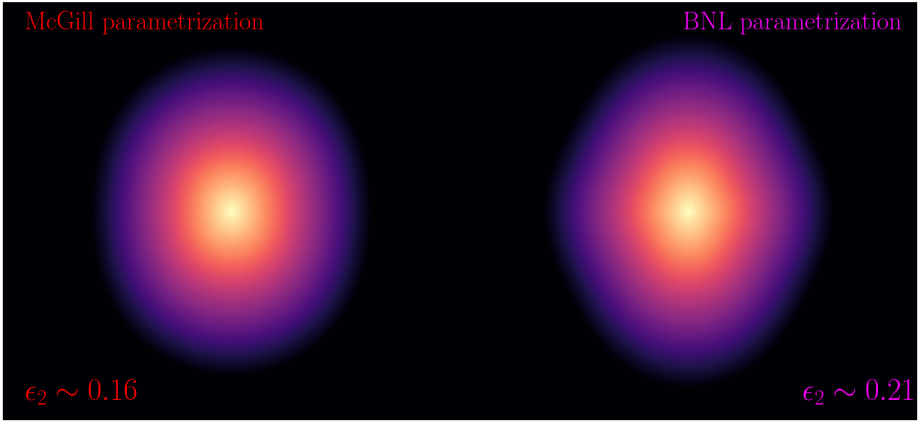

$R_0 = 6.874$ fm; a$= 0.556$ fm
$\beta_2 = 0.2802$; $\beta_4 = -0.0035$

$R_0 = 6.81$ fm; a$= 0.55$ fm
$\beta_2 = 0.28$; $\beta_4 = 0.093$

IP-Glasma Multiplicity Mechanisms

- The IP-Glasma model is based on the CGC framework. N_{coll} and N_{part} do not enter explicitly. Multiplicities are governed by the combination

$$\frac{Q_s^2 S_\perp}{\alpha_s}$$

with Q_s the saturation scale, $S_\perp$ the overlap area in the transverse plane and α_s the QCD coupling constant.

IP-Glasma Multiplicity Mechanisms

- The IP-Glasma model is based on the CGC framework. N_{coll} and N_{part} do not enter explicitly. Multiplicities are governed by the combination

$$\frac{Q_s^2 S_\perp}{\alpha_s}$$

For symmetric nuclei, $Q_s^2 \propto A^{1/3}$, while for deformed nuclei, $A^{1/3}$ is replaced with the average number of nucleons along the beam direction!

Importance of nuclear structure

Importance of nuclear structure

Nuclear structure determines the nuclear thickness function $T_{A(B)}$, which is a crucial early-stage quantity in initial state models like TRENTO and IP-Glasma

- TRENTO: $s(x,y) \propto \left[\frac{T_A^p + T_B^p}{2}\right]^{\frac{1}{p}}$
  - $\langle N_{CH} \rangle \propto \int s(x,y)dxdy$

Importance of nuclear structure

Nuclear structure determines the nuclear thickness function $T_{A(B)}$, which is a crucial early-stage quantity in initial state models like TRENTO and IP-Glasma

- TRENTO: $s(x,y) \propto \left[\frac{T_A^p + T_B^p}{2}\right]^{\frac{1}{p}}$
  - $\langle N_{CH} \rangle \propto \int s(x,y)dxdy$
- IP-Glasma: $\pi^2 \frac{xg}{N_c} \alpha_s \boldsymbol{T_A} = Q_s^2$
  - $\frac{xg}{N_c}$ is the gluon momentum density
  - α_s is the strong coupling constant
  - Q_s^2 is the saturation scale

Importance of nuclear structure

Nuclear structure determines the nuclear thickness function $T_{A(B)}$, which is a crucial early-stage quantity in initial state models like TRENTO and IP-Glasma

- TRENTO: $s(x,y) \propto \left[\frac{T_A^p + T_B^p}{2}\right]^{\frac{1}{p}}$
  - $\langle N_{CH} \rangle \propto \int s(x,y)dxdy$
- IP-Glasma: $\pi^2 \frac{xg}{N_c} \alpha_s \boldsymbol{T_A} = Q_s^2$
  - $\frac{xg}{N_c}$ is the gluon momentum density
  - α_s is the strong coupling constant
  - Q_s^2 is the saturation scale
    - $\langle N_{CH} \rangle \propto \frac{Q_s^2 S_\perp}{\alpha_s}$

Importance of nuclear structure

Nuclear structure **also** determines the overlap area $S_\perp$ of the two nuclei post-collision

Importance of nuclear structure

Nuclear structure **also** determines the overlap area $S_\perp$ of the two nuclei post-collision

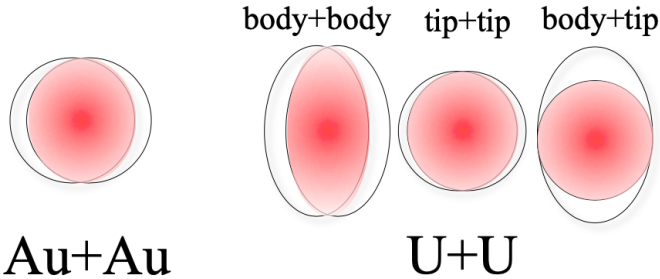

Importance of nuclear structure

Nuclear structure **also** determines the overlap area $S_\perp$ of the two nuclei post-collision

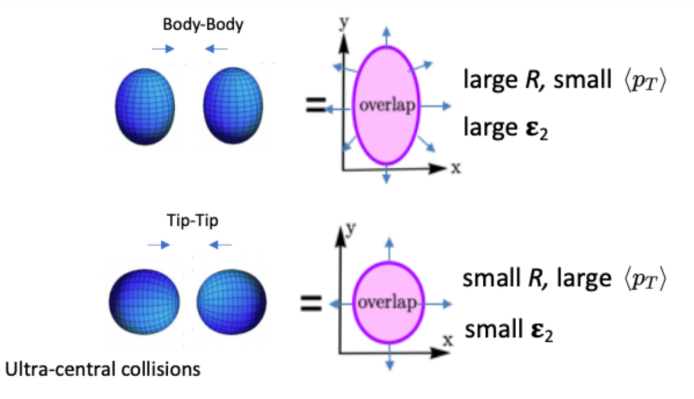

Figure from Giacalone, PRL 124, 202301 (2020)

Deformed Woods-Saxon Basics

The Woods-Saxon distribution is widely used in the field

Deformed Woods-Saxon Basics

The Woods-Saxon distribution is widely used in the field

$$\rho(r,\theta) = \frac{\rho_0}{1 + exp(\frac{R(\theta) - R_0'}{a})}$$

$$R(\theta) = R_0(1 + \beta_2 Y^{20}(\theta) + \beta_3 Y^{30}(\theta) + \ldots)$$

Deformed Woods-Saxon Basics

The Woods-Saxon distribution is widely used in the field

$$\rho(r,\theta) = \frac{\rho_0}{1 + exp(\frac{R(\theta) - R_0'}{a})}$$

$$R(\theta) = R_0(1 + \beta_2 Y^{20}(\theta) + \beta_3 Y^{30}(\theta) + \ldots)$$

- **Spherically symmetric:** $\beta_2 = \beta_3 = 0$

Deformed Woods-Saxon Basics

The Woods-Saxon distribution is widely used in the field

$$\rho(r,\theta) = \frac{\rho_0}{1 + exp(\frac{R(\theta) - R_0'}{a})}$$

$$R(\theta) = R_0(1 + \beta_2 Y^{20}(\theta) + \beta_3 Y^{30}(\theta) + \ldots)$$

- **Spherically symmetric:** $\beta_2 = \beta_3 = 0$
- **Deformed:** $0.05 \leq \beta_2 \leq 0.4$; $0.01 \leq \beta_3 \leq 0.3$; $0 \leq \beta_4 \leq 0.1$

Deformed Woods-Saxon Basics

The Woods-Saxon distribution is widely used in the field

$$\rho(r,\theta) = \frac{\rho_0}{1 + exp(\frac{R(\theta) - R_0'}{a})}$$

$$R(\theta) = R_0(1 + \beta_2 Y^{20}(\theta) + \beta_3 Y^{30}(\theta) + \ldots)$$

Example Parametrization[1]: $R_0 = 6.784$; $a = 0.0556$; $\beta_2 = 0.2802$; $\beta_4 = -0.0035$

1. H. De Vries, C.W. De Jager, C. Devries, Atomic Data (1987))

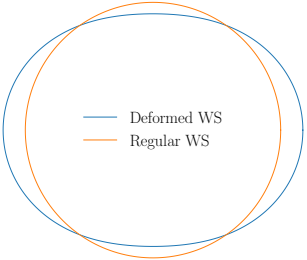

Deformed Woods-Saxon Basics

The Woods-Saxon distribution is widely used in the field

$$\rho(r,\theta) = \frac{\rho_0}{1 + exp(\frac{R(\theta) - R_0'}{a})}$$

$$R(\theta) = R_0(1 + \beta_2 Y^{20}(\theta) + \beta_3 Y^{30}(\theta) + \ldots)$$

Example Parametrization[1]: $R_0 = 6.784$; $a = 0.0556$; $\beta_2 = 0.2802$; $\beta_4 = -0.0035$

1. H. De Vries, C.W. De Jager, C. Devries, Atomic Data (1987))

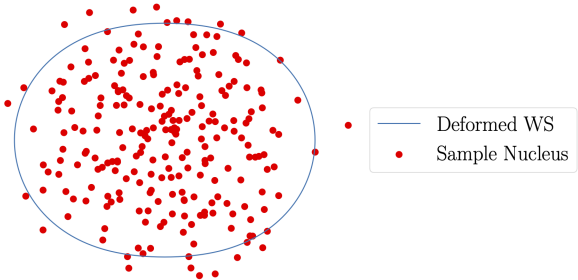

Deformed Woods-Saxon Basics

Other WS deformation parameters exist, such as the triaxiality parameter γ:

$$\rho(r,\theta) = \frac{\rho_0}{1 + exp(\frac{R(\theta) - R_0'}{a})}$$

$$R(\theta) = R_0(1 + \beta_2 \left[cos\gamma Y^{20}(\theta) + sin\gamma Y^{22}(\theta,\varphi) \right] + \beta_3 Y^{30}(\theta))$$

Deformed Woods-Saxon Basics

Other WS deformation parameters exist, such as the triaxiality parameter γ:

$$\rho(r,\theta) = \frac{\rho_0}{1 + exp(\frac{R(\theta) - R_0'}{a})}$$

$$R(\theta) = R_0(1 + \beta_2 \left[cos\gamma Y^{20}(\theta) + sin\gamma Y^{22}(\theta,\varphi)\right] + \beta_3 Y^{30}(\theta))$$

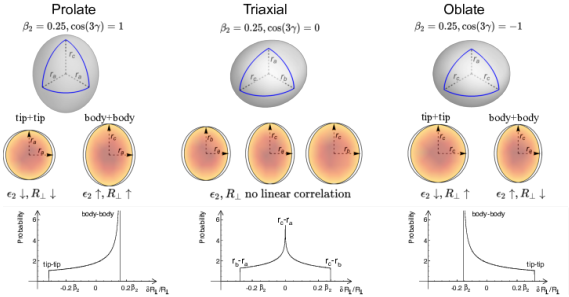

Figure from Jiangyong Jia, arXiv 2109, 00604 (2021)

Initial Condition

- Large-x partons serve as δ-function colour sources on the light cone (x^+ & x^-)

$$J^{\mu}_{A(B)}(x) = \delta^{\mu-(+)}\delta(x^{+(-)})\rho_{A(B)}(x)$$

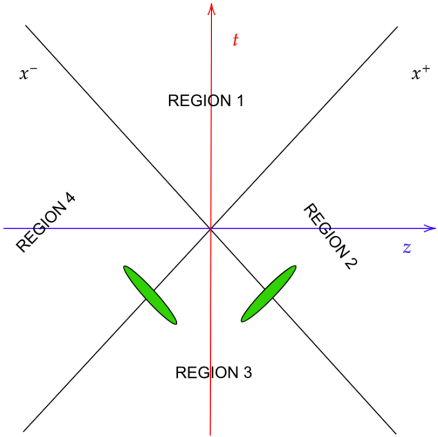

Initial Condition

- Large-x partons serve as δ-function colour sources on the light cone (x^+ & x^-)
- Fields in regions 2 & 4 are pure gauge

$$A_i^{A(B)} = \frac{i}{g} V \partial_i V^\dagger$$

$$A_\eta^{A(B)} = 0$$

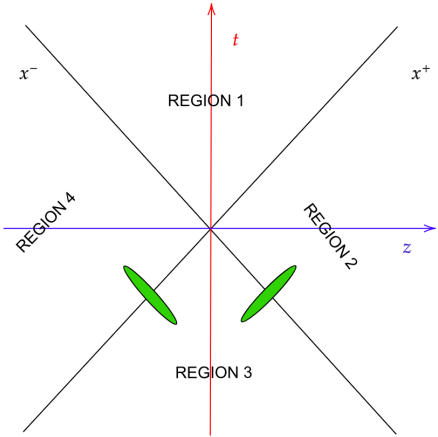

Initial Condition

- Large-x partons serve as δ-function colour sources on the light cone (x^+ & x^-)
- Fields in regions 2 & 4 are pure gauge
- Solution-matching on boundaries 1-4 and 1-2 provides solution for gauge fields in region 1

$$E^\eta = -ig\left[A^i_{(A)}, A^i_{(B)}\right]$$

$$A^i = A^i_{(A)} + A^i_{(B)}$$

$$A_\eta = 0$$

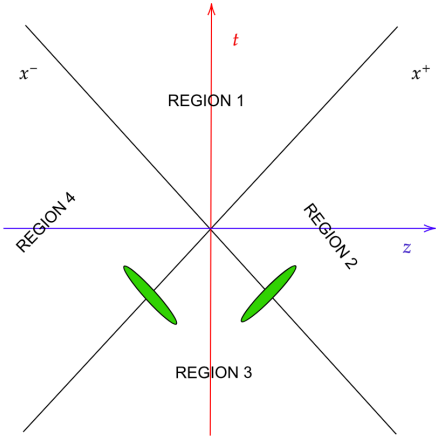

Hydrodynamics & Hadronization

Hydrodynamics: MUSIC

- Relativistic viscous hydrodynamics code
- Parametrization based on previous work (S. McDonald, C. Shen, F. Fillion-Gourdeau, S. Jeon, C. Gale, PRC (2017)):
  - Equation of state: HotQCD
  - $\tau_{sw} = 0.4$ fm
  - Constant shear viscosity $\frac{\eta}{S} = 0.12$
  - Bulk viscosity depends on temperature
  - Freeze-out temperature set to $T_{freeze} = 145 MeV$
  - Once every cell is frozen, move to hadronization

Hadronization: iSS + UrQMD

- Standard iSS + UrQMD parameters

Selecting Collision types

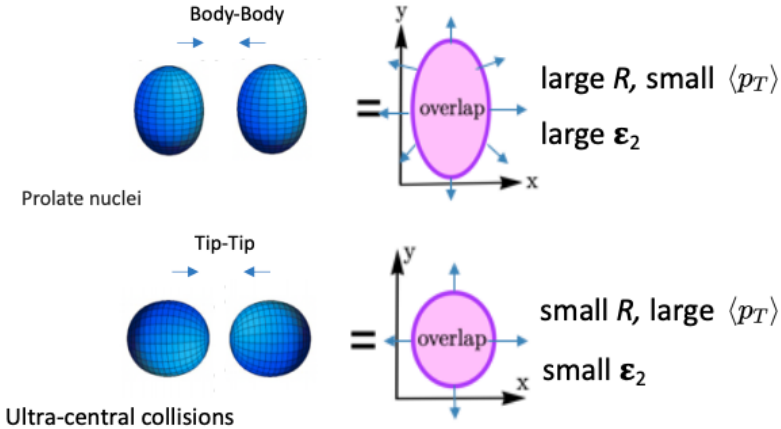

Figure from Giacalone, PRL124 (2020)

Selec

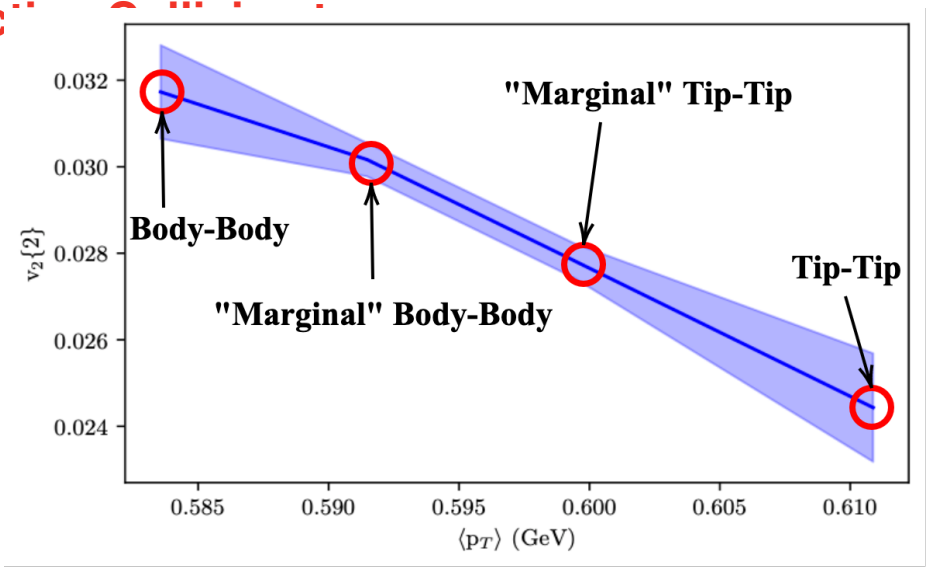

- Strong cuts in ZDC & scaled multiplicity enable body-body and tip-tip event selection
- Larger $v_2\{2\}$ (and overlap area) at smaller $\langle p_T \rangle$ means energy density is primary generator of p_T